A METHOD FOR QUICK ESTIMATION OF ENGINE MOMENT OF INERTIA BASED ON AN EXPERIMENTAL ANALYSIS OF TRANSIENT WORKING PROCESS

Predrag D. MRDJA [*]***, Nenad L. MILJIĆ, Slobodan J. POPOVIĆ, and Marko N. KITANOVIĆ***

Faculty of Mechanical Engineering, University of Belgrade, Belgrade, Serbia

Original scientific paper
https://doi.org/10.2298/TSCI170915224M

This paper presents an unconventional approach in a fast estimation of the overall engine inertia based on engine testing under transient condition (acceleration and deceleration) with simultaneous in cylinder working process analysis and friction losses estimation. The presented procedure is based on a single slow dynamic slope full load engine speed sweep test which, coupled with a simple lumped-mass engine dynamometer model, provides correct overall engine inertia estimation. Compared with the more conventional approaches in deriving information on engine inertia, besides its speed and accuracy, presented procedure provides more in depth information on both engine's dynamic response and friction as a surplus.

Key words: *internal combustion engine transient working process analysis, engine inertia, dynamic engine testing, engine friction losses*

Introduction

A typical automotive powertrain environment exploits the internal combustion (IC) engine in an extremely dynamic manner. Thus, engine processes transient behaviour has been in focus of research and optimization for years. Present and future ultimate goals in IC engine development, related almost exclusively to the fuel economy and exhaust emission improvement, can hardly be achieved without intensive dynamic testing of engines. Therefore, a full attention of IC engine researchers is given to the improvement of dynamic testing procedures, transient data analysis and reliable process information deduction. Engine transients can be characterized through single or simultaneous load and speed change of the engine. The latter, involving the engine speed change containing mechanical inertia related effects which, in overall, blurs the picture of the engine's working process itself. Hence, compensation and elimination of engine inertia issues is of great importance in transient working process analysis, and this can be achieved only by exact identification of engine mechanical inertia parameters.

In the last few years, the development of dynamic engine test procedures is in focus of numerous scientific research institutes, Universities and leading companies in the automotive industry. The main goal of those research endeavours is aimed at maximizing testing automation and therefore at reducing needed testing time and founds resources. During the powertrain development process, and especially during engine optimization for emission legislations, in-vehicle tests are the slowing factor [1, 2], and for that reason, most of the tests are transferred to the driving cycle highly dynamic engine test stands [3]. Dynamic engine testing has many

[*] Corresponding author, e-mail: pmrdja@mas.bg.ac.rs

advantages and disadvantages compared to the steady-state approach, but for some applications, the dynamic change of the engine operating point is an unavoidable condition. In general, simulation of a driving cycle represents certain changes with respect to engine load and speed over time. Usually, the engine speed is controlled in closed loop operation by the dynamometer control unit using the information of angular speed over the dyno angular speed encoder. On the other hand, engine torque is also controlled in the closed loop, relying on the torque meter (TM) or force transducer readings. At this point care must be taken regarding rotational movement elements and their mass moment of inertia influence [4, 5]. Because of variable engine speed during the driving cycle, the torque-measuring device will be affected by a particular amount of inertia-induced torque. Depending on the test-bed configuration, elements such as the engine, drive shaft and the dynamometer needs to be evaluated in terms of moment of inertia.

Conventional approach in obtaining info on the inertia of engine's moving parts is relying on previous knowledge and information from the designing stage of the engine itself or on a simple free engine deceleration test where subtle changes in engine friction and real engine working conditions influences are neglected. The motivation, behind the research presented in this paper, is drawn exactly upon the idea to overcome this issue and estimate engine overall moment of inertia in a fast manner but within the real operating conditions and full identification of the friction losses as well.

In this paper analysis will be conducted on results derived by means of a basic lumped-mass model of a system consisting of an engine's (and its axillaries) moving elements, drive shaft and dyno coupling, with a focus on TM readings as a source of system behaviour information.

Two different approaches of estimating the engine moment of inertia will be presented. The first method relies on statistical analysis of estimated inertia values by means of previously obtained steady-state engine experimental results. The second approach is based on iterative prediction of engine moment of inertia combined with minimization of friction losses hysteresis within the dynamic excitation. The obtained results are very similar using those methods, but the second one is recommended because less data is needed.

Table 1. Test-bed key sensor specification

Description	Sensor type
Engine speed	Optical encoder, AVL 365C
Engine torque	Torque sensor, HBMT40
Cylinder 1-4 pressure indicating	AVL GM12D + Micro IFEM Piezo Amp.

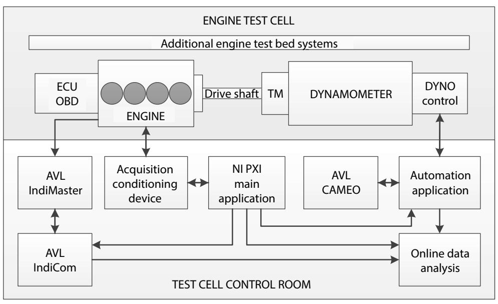

Figure 1. Engine test cell systems disposition and automation system configuration

Experimental installation

For the purpose of this experiment, the PSA DV4TD 8HT (1.4 l, 40 kW, 8 valves, compression ignition, turbocharged, non-intercooled version) engine was coupled with an AC dynamometer. Basic engine test-bed components and some of the measuring points are overviewed briefly in the fig. 2. Beside parameters available on the engine on-board diagnostics, the installation was equipped with additional measuring chains, where the key ones for the experiment are described in the tab. 1.

All time-resolved parameters were acquired using a multifunctional National Instruments NI PXI-6229 and NI PXI-6123 acquisition cards as a part of the NI PXI platform [6]. The engine was equipped with an optical

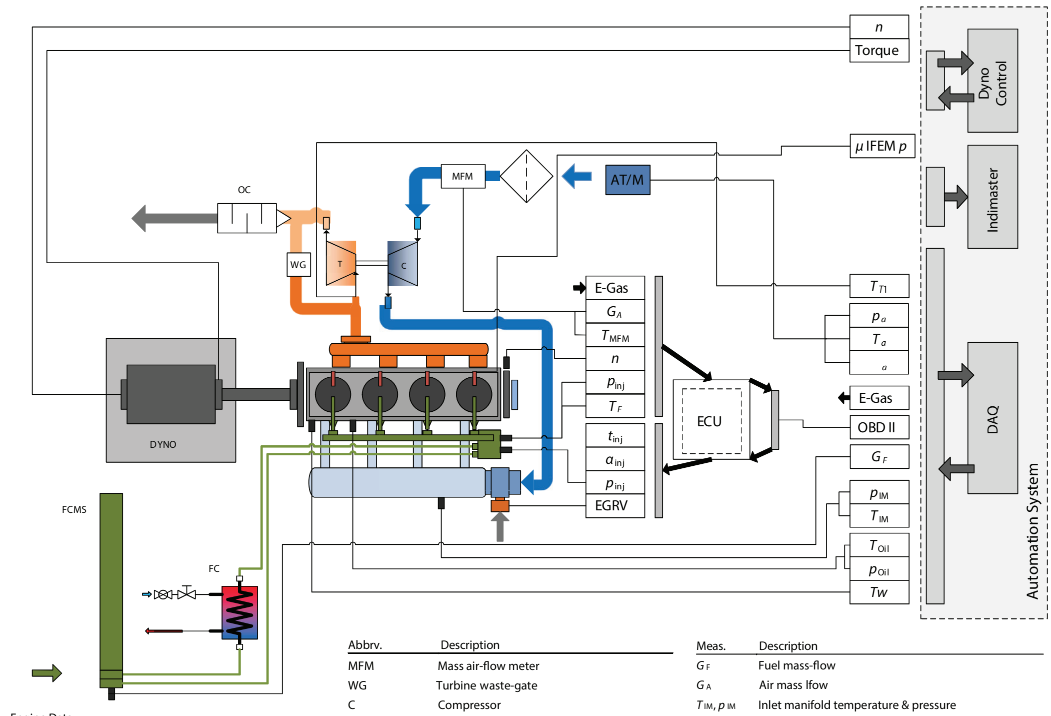

Engine Data	
Manufacturer	PSA group
Model	DV4TD 8HT
Type	CI; turbocharged, non-intercooled;
Bore	73.7 mm
Stroke	84.0 mm
Rated power	40 kW at 4000 min^{-1}
Rated Torque	130 Nm
Fuel injection system	Common rail
Turbocharger	KP35 (3K-BW)
Bore	73.7 mm
Stroke	84.0 mm

Abbrv.	Description
MFM	Mass air-flow meter
WG	Turbine waste-gate
C	Compressor
OBD	On-board diagnostic interface
T	Turbine
EGRV	Exhaust gas recirculation valve
FC	Fuel conditioner
FCMS	Fuel consumption measurement system
DYNO	AC dynamometer
E-Gas	Engine torque demand control
OC	Oxi-cat
µ IFEM p	Amplifer for piezo-electric in-cylinder pressure transducers
AT/M	Atmospheric measurement module
ECU	Engine electronic control unit

Meas.	Description
G_F	Fuel mass-flow
G_A	Air mass lfow
T_{IM}, p_{IM}	Inlet manifold temperature & pressure
p_{inj}, α_{inj}	Fuel injection pressure & start of injection angle
t_{inj}	Fuel injection duration
T_{T1}	Turbine inlet temperature
T_{Oil}, p_{Oil}	Oil temperature & pressure
T_w	Engine coolant temperature
T_a, p_a, φ_a	Atmospheric air temperature, pressure and humidity

Figure 2. Engine test-bed disposition

incremental encoder and with piezoelectric pressure transducers on all four cylinders. Rest of the in-cylinder pressure indication system was completed with AVL charge amplifiers coupled with an embedded hardware platform for engine indicating [7], the AVL IndiModule 621. The AVL IndiCom [8] software solution has been used for engine indicating data visualization, measuring, and data manipulation. For defining the control sequence and setting the dynamic regime, the AVL CAMEO [9] software has been used, while a mediator in Modbus communication between CAMEO and the dynamometer control module has been in-house developed NI LabVIEW [10] application. A test bench schematic, along with the essential data flow between components is shown in the fig. 1.

Test procedure

The conducted experiment was very short, similar to those performed by Godburn *et al*. [11]. Engine speed was swept in two predefined cycles with gradients of ±5.59 rad/s^2 and ±16.06 rad/s^2, respectively, with ramp periods of 15 seconds in both cases. The main idea was to vary engine speed over time in a predefined cycle. Precisely, the engine was accelerated with a constant gradient from 1200 to 2000 min^{-1} in the first run, and from 1200 to 3500 min^{-1} in the second one, with a ramp period of 15 seconds in both cases. After reaching maximal engine speed, 10 seconds stabilization time was applied followed by engine speed decrease back to 1200 min^{-1} in both cases. In other words, applied angular accelerations/decelerations were equivalent to ± 5.59 rads^2 and ± 16.06 rads^2 in performed engine runs.

During tests, full engine load was applied with the idea to avoid influence of torque PID controller settings on engine torque fluctuations and thus TM readings. In addition, increased indicated mean effective pressure (*IMEP*) will lead to a more significant difference between the brake and friction parameter readings caused by engine friction losses and impact of inertia-inducted forces.

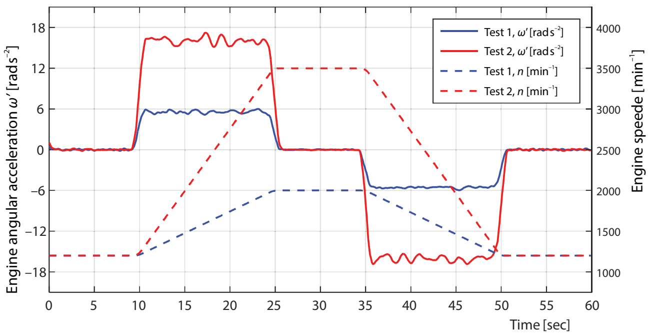

Figure 3. Experimental test cycle profiles; engine angular acceleration ω' rad/s^2 and engine speed n min^{-1} change over the time (*for color image see journal web site*)

Obtained engine speed, n [min^{-1}] and acceleration profiles, ω' [rad s^{-2}] for both tests are shown in the fig. 3. During the tests, engine speed demand towards the test bed automation system was updated at 50 times per second rate.

Data processing

All time-domain test-bed sensors readings were acquired using a sample rate of 500 Hz, while engine indicating was performed with an angular encoder resolution of 0.1 °CA. Evaluation of pressure traces and determination of *IMEP*, heat release, peak pressure angular location, maximum gradient of pressure trace and its angular location were determined on a cycle basis using real time processing capabilities of the AVL IndiMaster acquisition platform. Due to the known values of cycle duration, all angular and cycle-based values were transferred in the time domain using convenient scripts in AVL Concerto data post processing environment. Event synchronization check was applied, all channels were processed using a one second buffer moving average filter and resampled to a 10 Hz time base. The brake mean effective pressure (*BMEP*) and *IMEP* values are shown in the fig. 4 as functions of time and engine speed.

It is noticeable that a hysteresis is present in recorded data during the engine speed change, *i. e.* during the engine transient operating regime. As expected, the *BMEP* hysteresis is greater for more aggressive engine accelerations and decelerations. This observation is applicable for any other effective parameter change during the dynamic engine testing cycle.

Presence of *BMEP* hysteresis, shown in the fig. 4, is in direct relation to the value of the engine mass moment of inertia and the type of dynamic excitation of the system. It is noticeable that the ratio of *BMEP* hysteresis of both tests roughly follows the ratio of applied engine speed gradients and, accordingly, induced inertia torques. As a consequence, during a variable engine speed dynamic test this *BMEP*, *i. e.* torque offset has to be compensated during measurements and this can be done properly only by knowing the proper value of overall presented engine inertia.

For the sake of further analysis, the hysteresis of *IMEP* will be treated as negligible. Sound reasons for such an approach can be derived from the simplified analysis of a linear first-order system response under symmetric ramp excitation [12]. Upon a ramp excitation, the first-order system response is constantly below the steady-state level line, *i. e.* an offset response is evident. Changing the excitation ramp sign causes the sign change of the offset response also. If the system time constant is considerably slower than excitation ramp time, than the response offset is small enough and can be neglected. Moreover, by applying a symmetric ramp, with the same but opposite gradients, complete compensation of the response offset can be expected. A *slow enough* excitation ramp is a key element of the slow dynamic slope (SDS) testing methodology which is used for quasi-stationary measurements [13]. Figure 5(a) shows an example of gathered engine response by applying constant speed torque ramp excitation through the SDS approach. It can be seen that the response hysteresis depends on the system time constant. Variables heavily influenced by process inertia have much larger hysteresis than fast responding ones. Figure 5 (b) shows how fast the response of *IMEP* is with a SDS cycle duration of only 120 seconds. This provides a conclusion that even faster ramps could be applied with negligible offset expectation.

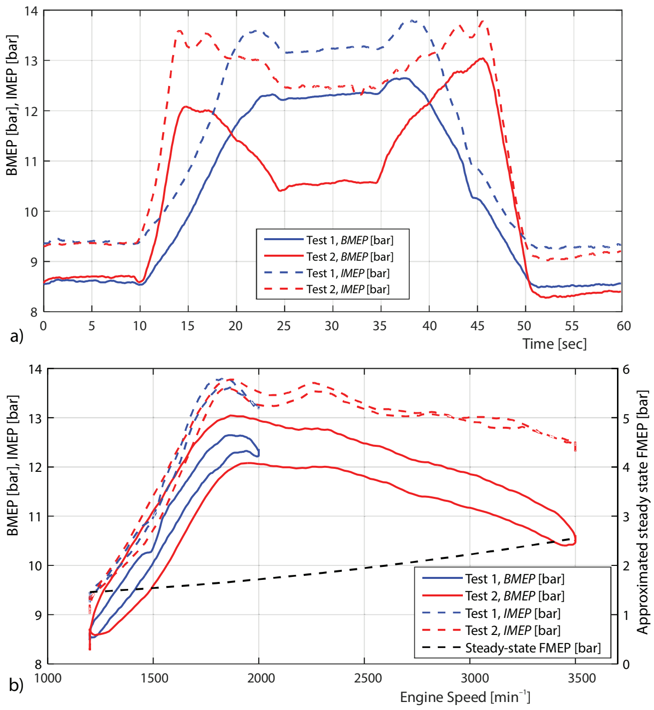

Figure 4. Measured *BMEP* and *IMEP*; (a) change in a time, (b) engine speed domain
(*for color image see journal web-site*)

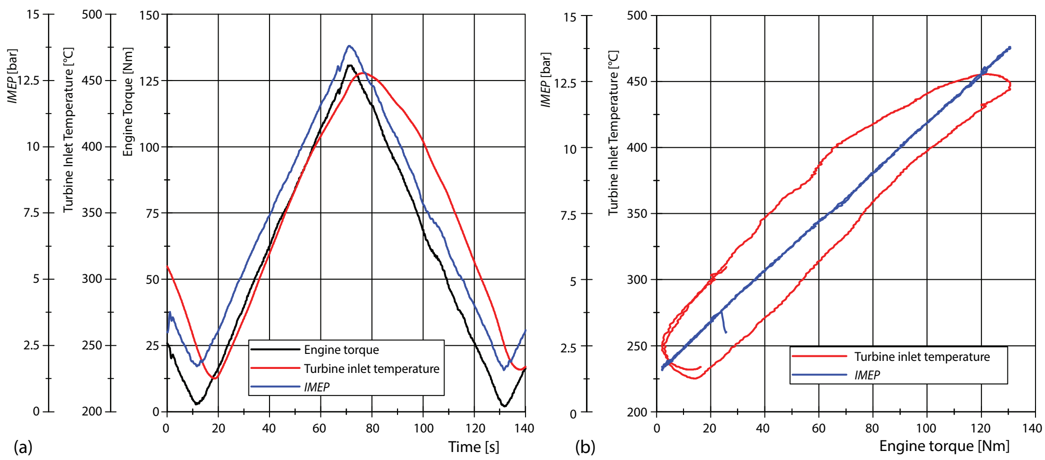

Figure 5. A dynamic engine testing procedure based on SDS methodology; engine response from symmetric torque ramp sweep in duration of 120 seconds at 2500 min^{-1}

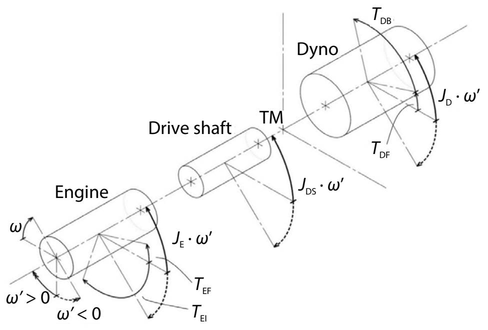

Figure 6. Schematic presentation of the simplified lumped-mass model of the engine test-bed system

Engine torque measurement – theoretical aspects

For further analysis, a simplified lumped-mass model of engine test-bed installation consisting of the engine (E), the drive shaft (DS), and the dynamometer (D) is presented in the fig. 6 and described in the tab. 2. Rotational masses oppose angular acceleration, ω', with the momentum caused by the moment of inertia of named elements (J_E, J_{DS}, J_D) in the opposite direction of angular acceleration. Dynamometer and drive shaft suppliers usually provide information about moment of inertia, in particular: $J_{DS} = 0.1$ kgm^2 and $J_D = 0.65$ kgm^2.

Table 2. Symbols related to fig. 6

Name	Description	Comment
T_{EI}	Indicated engine torque	Measured value. Depends on operating point stabilization
T_{EF}	Engine friction losses	Unknown value for dynamic regimes
T_{DF}	Dynamometer friction losses	Unknown value with negligible impact
T_{DB}	Dynamometer brake torque	Unknown value (possible indirect calculation)
TM	Torque meter device	Measured value. The difference between generated torque of two machines (engine and the dynamometer)
J_E	Engine moment of inertia	Required value (scalar). Does not depend on operating point stabilization
J_{DS}	Drive shaft moment of inertia	A known value
J_D	Dynamometer moment of inertia	A known value
ω'	Engine angular acceleration	Measured value

The dyno friction losses torque, T_{DF}, is negligible in our case, but generally exists and mainly depends on the angular speed, ω. For the majority of modern engine testing installations, the value of effective dynamometer braking torque, T_{DB}, is internally controlled. The sum of T_{DF} and T_{DB} torque is measured using a shaft-mounted TM or a housing mounted force transducer and it is possible to assign this value to the engine effective torque, but only in steady--state operating conditions in terms of angular acceleration ω', thus $\omega' = 0$ rad/s^2.

In the general case, the following equation of the system's rotational motion and momentum equilibrium could be written:

$$T_{EI} - T_{EF} - T_{DB} - T_{DF} - \left(J_E + J_{DS} + J_D\right)\omega' = 0 \tag{1}$$

The torque values on each side of the TM can be expressed:

$$T_{TM} = T_{EI} - T_{EF} - \left(J_E + J_{DS}\right)\omega' \tag{2}$$

$$T_{TM} = T_{DB} + T_{DF} + J_D\,\omega' \cong T_{DB} + J_D\,\omega' \quad | T_{DF} \cong 0 \tag{3}$$

There is a certain limit concerning the maximal value of the dynamometer acceleration that depends on the maximum AC machine applied torque and its moment of inertia in addition to:

$$J_{\mathrm{E}} = \frac{T_{\mathrm{EI}} - T_{\mathrm{EF}} - T_{TM}}{\omega'} - J_{\mathrm{DS}} \quad | \, \omega' \neq 0 \tag{4}$$

The unknown variable in the eq. (4), which is needed for the direct calculation of engine moment of inertia, J_{E}, is the value of the engine friction losses torque, T_{EF}, obtained in dynamic conditions as specified by the experiment set-up. Values of indicated engine torque, T_{EI}, and TM readings, T_{TM}, are obtained from *IMEP* and *BMEP* sweeps shown in fig. 4.

In order to overcome the lack of information regarding the T_{EF}, the results of steady-state engine testing were used. The difference between the brake and indicated parameters, which resulted in engine friction losses torque T_{EF}^{SS} has been approximated using steady-state data.

$$T_{\mathrm{EF}}^{\mathrm{SS}} = T_{\mathrm{EI}}^{\mathrm{SS}} - T_{\mathrm{TM}}^{\mathrm{SS}} \qquad \Rightarrow \qquad J_{\mathrm{E1}} = \frac{T_{\mathrm{EI}} - T_{\mathrm{EF}}^{\mathrm{SS}} - T_{TM}}{\omega'} - J_{\mathrm{DS}} \qquad | \, \omega' \neq 0 \tag{5}$$

Should be kept in mind that in eq. (5), measured torque, T_{TM}, has a hysteresis while used steady-state effective torque values, $T_{\mathrm{EF}}^{\mathrm{SS}}$, belong to a line which is close to the mean value line of the T_{TM} hysteresis shape. Also, in the experiment, hysteresis envelopes are responses to an engine acceleration/deceleration which is far from perfectly constant, fig. 3, due to the nature of involved test bed automation system features and downsides [9]. This slight deviation of acceleration/deceleration from constant steady-state, implies solutions of eq. (5) to be spread around its mean value. Hence, solutions of J_{E1} are concentrated within two distinctive data clouds on each side of the acceleration/deceleration ramp, fig. 7(a). Figure 7(b) shows a frequency distribution of the solutions for J_{E1} with an evident strong influence of acceleration/deceleration intensity on the solutions distribution width. The focus of the analysis is put on the mean value of the solution data cloud – $\bar{J}_{\mathrm{E1}}$ as indicative estimates.

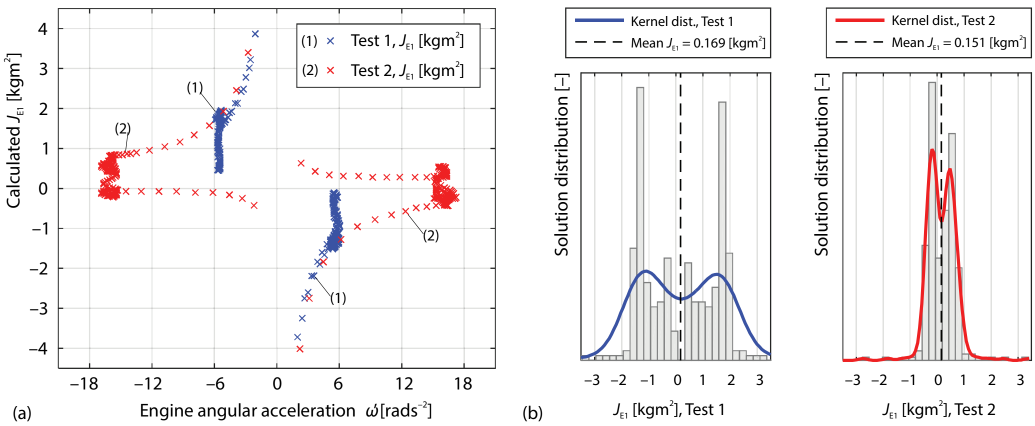

Figure 7. Engine moment of inertia solution distribution and mean value for approximated engine friction losses by means of steady-state testing results

The identified value of the mean moment of inertia of the engine, by using the above-mentioned approach, is within the range for a given class of engines and close enough to the correct value. On the other side, the method's drawback is in relaying on already gathered steady-state data which is a time-consuming precondition.

The second approach for obtaining the engine moment of inertia is based on the exclusive analysis of dynamically gathered engine testing results. Because the change of engine friction losses, T_{EF}, over time is unknown in dynamic operation, the calculation is carried in the opposite direction. In this case, the engine moment of inertia was iteratively assumed and then the dynamic friction losses were calculated. Additional assumptions were included, such as that the change of engine friction losses does not depend on the engine angular acceleration, which is shown in eq. (6):

$$T_{\mathrm{EF}} \neq f(\omega') \tag{6}$$

Figure 8 shows the change of the calculated dynamic friction mean effective pressure (*FMEP*), and its smoothing spline approximation, in time and engine speed domain for the conducted dynamic tests and assumed the engine moment of inertia $J_{\mathrm{EA}} = 0$ kgm^2. In that sense, predicted *FMEP* is calculated using eq. (7) and taking into account previous assumptions and engine displacement V_{E} dm^3:

$$FMEP_{\mathrm{predicted}} = IMEP - BMEP - (J_{\mathrm{EA}} + J_{\mathrm{DS}})\omega' \frac{\pi}{V_{\mathrm{E}} 25} \tag{7}$$

This value is incorrectly selected with the intention of presenting its impact on T_{EF} results. The presence of *FMEP* hysteresis is noticeable in the fig. 8 (b) and it is in direct relation with the engine angular accelerations and deceleration periods during the tests. The condition described in eq. (6) provide further analysis based on the approximation of dynamic *FMEP* over the engine angular speed. In other words, the minimization of the sum of square error (*SSE*) of the mentioned approximation would lead to the correct result.

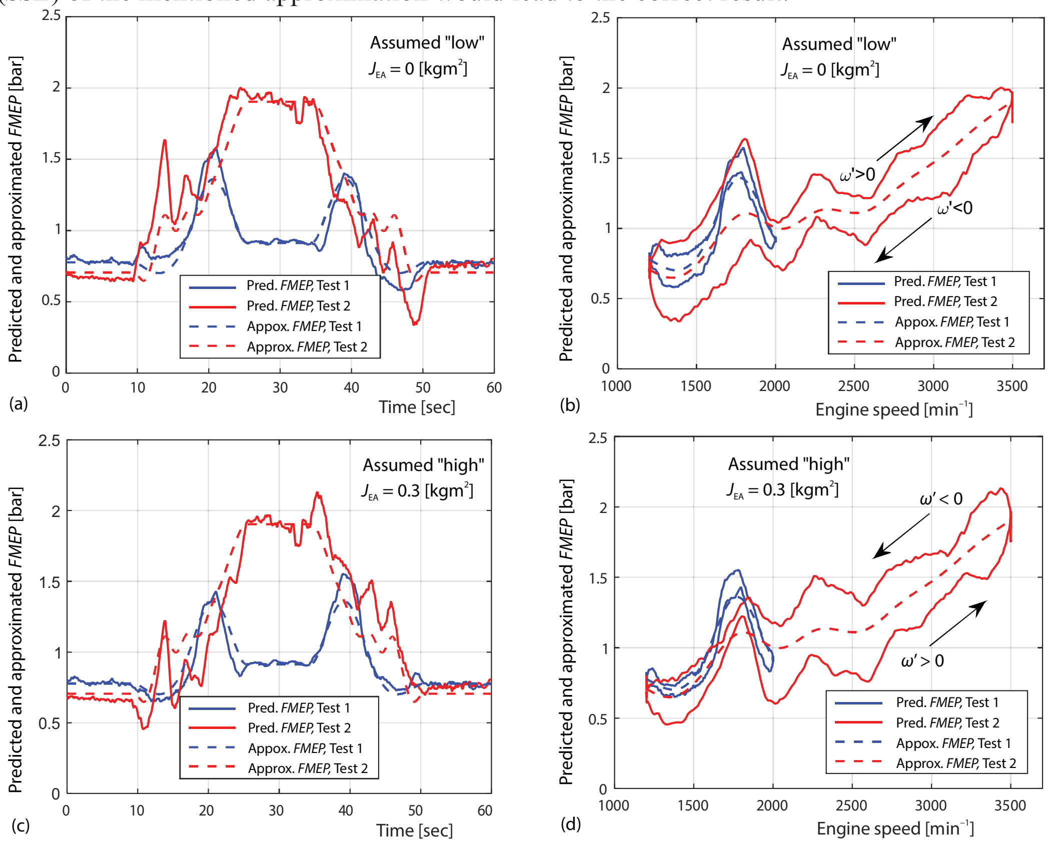

Figure 8. Estimated dynamic *FMEP* for various assumptions of engine moment of inertia; too low / high in time (a / c) and speed domain (b / d) (*for color image see journal web site*)

A similar case is presented in figs. 8(c) and 8(d), except that another extreme value of too high assumed engine moment of inertia is chosen. It is evident that the calculated values for *FMEP* within dynamic conditions have the opposite direction for positive and negative engine speed slopes comparing with fig. 8(b).

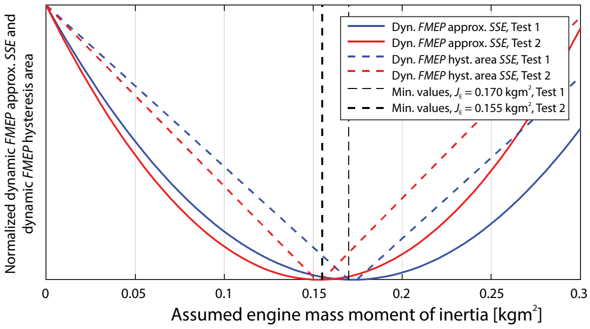

Figure 9. The *SSE* of *FMEP* approximation in dynamic conditions and the minimal value of *SSE* indicates a correct estimation of engine moment of inertia (*for color image see journal web site*)

Beside introduction and evaluation of approximation error, good indicator of correctly selected engine inertia could be drawn out from hysteresis area calculation. Minimisation of hysteresis area, which is shown in the figs. 8 and 9, will lead to flip-point of predicted *FMEP* lines for positive and negative angular accelerations. Results obtained by those two approaches are very similar, but additional data manipulation is required because of unequal data sampling in the engine speed domain. In addition, the iterative estimation of engine moment of inertia is performed and the change of dynamic *FMEP* smoothing spline approximation *SSE* is given in fig. 9 for both conducted tests.

It can be noticed that the best fit of *FMEP* during transient engine speed change corresponds to a minimal value of *SSE* which is calculated using eq. (8):

$$SSE\left(J_{\mathrm{EA}}\right)=\sum_{s=1}^{NS}\left[FMEP_{\mathrm{predicted}}(s)-FMEP_{\mathrm{aprox}}(s)\right]^{2} \tag{8}$$

where NS represent the total number of samples during the experiment.

Experimental results comparison with CAD model evaluation

For the purpose of results validation, a detailed CAD model of main engine rotational elements was made. Engine component masses and their corresponding moment of inertia are presented in the tab. 3. However, it should be noted that the total value is slightly underestimated because elements such as the camshaft, pulleys, common rail fuel pump, alternator, the coolant pump impeller and various belts were not modelled.

Table 3. Moment of inertia of main engine elements gathered from CAD models

Engine part name	Engine part mass [g]	Engine part moment of inertia [kgm^2]
Crankshaft	12940	0.0192
Flywheel	7960	0.0742
Flywheel-drive shaft adapter	2800	0.0258
Connecting rod mass reduced to the crankpin journal	361.9	0.0024 (all 4 cylinders)
Inertia of the crankshaft mechanism oscillating parts		0.0022 (all 4 cylinders)
Poly-V pulley	2070	0.0069
Total		0.1307

Described experimental estimation of the engine moment of inertia takes into account the influence of engine fluids' inertia (coolant, oil, intake air and exhaust gas-flow in the dynamic condition) which is in non-linear relation to the engine speed and thus not presented in eqs. (5) or (7). In order to provide more accurate results, obtained estimations should be corrected having in mind the abovementioned statement. When compared to the CAD model based calculation it is evident that the dynamically estimated inertia is a bit higher with offsets dependable on engine speed ramp. These offsets could be designated:

$$\begin{aligned} \mathit{\Delta} J_{\mathrm{E1}} &= J_{\mathrm{E1}} - J^{*} \\ \mathit{\Delta} J_{\mathrm{E2}} &= J_{\mathrm{E2}} - J^{*} \end{aligned} \tag{9}$$

where J^{*} represents the correct value of the engine inertia, and indexes 1 and 2 are related to the slower and faster engine speed gradient, respectively.

By assuming that offsets from eq. (9) are related to the inertia of engine fluids' mass--flow and internal discharge losses and by using some analogies from the fundamental fluid mechanics equations we can also assume the correctness of the following relation:

$$\frac{\mathit{\Delta} J_{\mathrm{E1}}}{\mathit{\Delta} J_{\mathrm{E2}}} \approx \frac{\bar{Q}_2}{\bar{Q}_1} \approx \sqrt{\frac{k_2}{k_1}} \tag{10}$$

where $\bar{Q}$ represents the mean value of the engine fluids' flow during the acceleration ramp and k accompanying engine speed ramp gradient.

System of eqs. (9) and (10) have a single pair of solutions for the correction offsets:

$$\Delta J_{\mathrm{E2}} = \frac{\left(J_{\mathrm{E1}} - J_{\mathrm{E2}}\right)\left(1 + \sqrt{\dfrac{k_2}{k_1}}\right)}{\dfrac{k}{k_1 - 1}} \tag{11}$$

For the parameters used in the experiment, where k_1 and k_2 were, respectively, 5.59 and 16.06 rad/s^2 and initial estimations of the engine inertia were (from fig. 12) $J_{\mathrm{E1}} = 0.170$ and $J_{\mathrm{E2}} = 0.155$ kgm^2, the offset resulting from the equation 11 is $\mathit{\Delta} J_{\mathrm{E2}} = 0.0216$ kgm^2 which in turn provides a more accurate estimation of the mean engine moment of inertia:

$$J^{*} = J_{\mathrm{E2}} - \Delta J_{\mathrm{E2}} = 0.133\,\mathrm{kgm}^2 \tag{12}$$

Corrected estimation from eq. (12) is in very good agreement with the CAD based estimation which implies that short transient dynamic measurement can provide the value of engine inertia with remarkable accuracy.

Conclusion

Two methods for experimental estimation of the engine's moment of inertia are presented in this paper, where both of them are tested with two different engine operation cycles. The first approach presupposes knowledge of engine friction losses values from steady-state operating points, assuming that those values are identical during stationary and dynamic engine examination. The second approach requires far less data and thus, less time on the engine test bed. The assumption that was introduced implies that the value of engine friction losses during dynamic tests does not depend on engine angular acceleration. Results obtained using the second approach differs between 0.5% and 2.5% compared with the results of the first one. These deviations would be much smaller that the experiment was repeated several times. An introduction of an additional method for the correction of engine speed dependable non-linearities provided the final estimation of the mean engine inertia in a very good agreement with the CAD based model estimation. General recommendation for this type of experiment is to vary engine speed as fast as possible in order to achieve higher inertia inducted torques, taking into account the acceleration that the engine can handle and required dynamometer power for such a run.

Nomenclature

J – moment of inertia, [kgm^2]
k – acceleration/deceleration ramp gradient
NS – number of samples
Q – equivalent fluid-flow of all engine fluids
T – torque, [Nm]
V – volume, [dm^3]

Greek symbols

Δ – difference
ω – angular speed, [rads^{-1}]
ω' – angular acceleration, [rads^{-2}]

Subscripts

D – dynamometer
DB – dynamometer brake
DF – dynamometer friction
DS – drive shaft
E – engine
EF – engine friction
EI – engine indicated
TM – torque meter

Superscrips

* – new value
SS – steady-state

References

[1] Perez, F., *et al.*, Vehicle Simulation on an Engine Test Bed, *Proceedings*, SIA International Conference, *Diesel Engines – The Low CO$_2$ & Emissions Reduction Challenge*, 2008
[2] Burette, G., *et al.*, Vehicle Calibration Optimization Using a Dynamic Test Bed with Real Time Vehicle Simulation, *Proceedings*, Diesel Engines - Facing the Competitiveness Challenges, Campus INSA de Rouen, France, 2010
[3] Isermann, R., *Engine Modeling and Control: Modeling and Electronic Management of Internal Combustion Engines*, Springer, New York, USA, 2014
[4] Zweiri, Y. H., *et al.*, Detailed Analytical Model of a Single-Cylinder Diesel Engine in the Crank Angle Domain, *Journal of Automobile Engineering*, *215*, (2001), 11, pp. 1197-216
[5] Souflas, I., *et al.*, Dynamic Modeling of a Transient Engine Test Cell for Cold Engine Testing Applications, *Proceedings*, ASME 2014 International Mechanical Engineering Congress and Exposition, ASME, Montreal, Que., Canada, 2014
[6] Mrdja, P., Integrated Solution for Internal Combustion Engine Test Bench Control, Data Acquisition and Engine Control Unit Calibration, *Proceedings*, NIDays 2011 International Conference, Belgrade, 2011
[7] Paulweber, M., Lebert, K., *Powertrain Instrumentation and Test Systems: Development – Hybridization – Electrification*, Springer, New York, USA, 2016
[8] *** AVL Indicom Indicating Software v1.6. AVL List GmbH, Graz, Austria
[9] Dinić, S., *et al.*, Light Vehicles Test Procedures on an Automated Engine Test Bed, *Proceedings*, 17th Symposium on Thermal Science and Engineering of Serbia, Sokobanja, Serbia, 2015, pp. 1056-1061
[10] Petrović, V., *et al.*, Software and Hardware Challenges of Engine Test Bed Automation – Example of FME ICED Lab, *Proceedings*, 17th Symposium on Thermal Science and Engineering of Serbia, Sokobanja, Serbia, 2015, pp. 1062-1065
[11] Godburn, J., *et al.*, Computer-Controlled Non-Steady-State Engine Testing, *International Journal of Vehicle Design*, *12* (2001) 1, pp. 50-60
[12] Schreiber, A., Dynamic Engine Measurement with Various Methods and Models, (in German), in *Electronic Management of Motor Vehicle Powertrains*, Springer, Berlin, German, 2010, pp. 167-199
[13] Ward, M. C., *et al.*, Investigation of Sweep Mapping Approach on Engine Testbed, *Proceedings*, SAE 2002 World Congress & Exhibition, Detroit, Mich., USA, 2002

Paper submitted: September 15, 2017
Paper revised: October 16, 2017
Paper accepted: October 24, 2017